

Modeling Battery Swapping Stations for Sustainable Urban Mobility

Original

Modeling Battery Swapping Stations for Sustainable Urban Mobility / Renga, Daniela; Meo, Michela. - In: SUSTAINABLE ENERGY, GRIDS AND NETWORKS. - ISSN 2352-4677. - 41:(2025), pp. 1-11. [10.1016/j.segan.2024.101592]

Availability:

This version is available at: 11583/2995351 since: 2024-12-19T11:34:12Z

Publisher:

Elsevier

Published

DOI:10.1016/j.segan.2024.101592

Terms of use:

This article is made available under terms and conditions as specified in the corresponding bibliographic description in the repository

Publisher copyright

Elsevier postprint/Author's Accepted Manuscript

© 2025. This manuscript version is made available under the CC-BY-NC-ND 4.0 license
<http://creativecommons.org/licenses/by-nc-nd/4.0/>. The final authenticated version is available online at:
<http://dx.doi.org/10.1016/j.segan.2024.101592>

(Article begins on next page)

Modeling Battery Swapping Stations for Sustainable Urban Mobility

Daniela Renga^a, Michela Meo^a

^aDepartment of Electronics and Telecommunications, Politecnico di Torino, Corso Duca degli Abruzzi 24, Torino, 10129, Italy

Abstract

With the road transportation alone being responsible of almost half the total oil demand over all sectors, electric vehicles (EVs) represent a promising solution to address sustainability concerns raised by urban mobility. However, a sustainable and pollution-free EV charging process cannot be enabled without an extensive penetration of Renewable Energy (RE) sources and a pervasive deployment of smart charging scheduling approaches. In a similar scenario, renewable powered Battery Swapping Stations (BSSs) can play a key role to enable sustainable and feasible electric mobility (e-mobility). Considering an on-grid BSS, additionally powered by photovoltaic panels, we analyze the proper dimensioning of its capacity in terms of number of sockets and the proper sizing of the RE supply to satisfy the battery swapping demand, trading off cost, Quality of Service (QoS) and feasibility constraints. We propose an analytical model to represent the BSS operation and limit the complexity of system investigation, exploring its potentiality to dimension the BSS system based on the actual battery swapping demand. Our findings highlight how integrating a local RE supply allows to considerably decrease cost by almost 40%. Furthermore, in the planning and deployment of BSS systems, the model results effective in finding good tradeoffs among QoS requirements, capital expenditures, and operational cost.

Keywords: Battery Swapping Stations, e-mobility, Renewable Energy, Queuing Model

Email addresses: daniela.renga@polito.it (Daniela Renga),
michela.meo@polito.it (Michela Meo)

1. Introduction

Nowadays the transportation sector heavily relies on oil as the main energy source, granting more than 90% of the total energy demand. Moreover, unlike other sectors, the road transportation has kept increasing its oil demand over years, with almost a three fold increase in less than five decades [1]. Indeed, with almost 2000 Mtoe per year, the road transportation alone accounts for almost almost 50% of the total oil consumption over all sectors, hence raising remarkable sustainability concerns [1].

In addition, air pollution represents a further alarming issue related to traditional transportation, hence boosting the adoption of electric vehicles (EVs) particularly in urban scenarios. Nevertheless, the potential benefit of e-mobility in terms of pollution reduction is not straightforward. Indeed, it requires, on the one hand, an extensive integration of Renewable Energy Sources (RES) in the supply systems to charge the EV batteries, and, on the other hand, the proper implementation of smart scheduling strategies to efficiently manage the EV battery recharge process.

The transition from traditional Battery Charging Stations towards the Battery Swap (BS) technology has the potential to enable an easier deployment of sustainable and smart charging solutions. A BS based charging station entails EVs equipped with batteries that can be easily and rapidly replaced with a fully charged battery once they are discharged. Hence, the operation of Battery Swapping Stations (BSSs) results comparable to a fuel filling station, since the battery charging service is decoupled from the EV mobility service, and can be offered and managed by independent companies owning the BSSs. Several advantages derive from the BS technology based approach with respect to the standard e-mobility, starting from the limitation of the range anxiety (fear that an EV has insufficient range to reach the destination), representing a major obstacles to the large-scale penetration of EVs [2, 3, 4]. Indeed, the time required to swap an EV battery is comparable to the time to refuel an Internal Combustion Engine (ICE) vehicle. Furthermore, novel business models can be conveniently introduced. According to a *Battery-as-a-Service* paradigm, the EVs may be owned by private users or by a car sharing company, whereas a separate provider owning the battery pool is responsible of managing the charge, distribution and maintenance of the batteries. The cost for purchasing an EV is hence reduced, saving the EV owners the cost faced for battery replacement at the end of its lifetime. In addition, the implementation of dynamic charging scheduling algorithms is facilitated, since no strict constraints are posed on the recharging process, that can hence be modu-

lated based on the varying RES availability. Finally, the interaction with the Smart Grid (SG) can be enhanced entailing mutual benefits for the SG operator and the battery provider, since the EV battery charging can be properly scheduled when electricity prices are lower, or when RE is available, or it can be more effectively postponed and resumed to avoid to overload the electric grid and meet various SG requirements.

Following our previous study presented in [5], in this paper we focus on urban e-mobility based on battery swap technology, considering a renewable powered BSS. We extend the analysis about properly dimensioning the BSS capacity and the RE supply to trade off cost and Quality of Service (QoS). In addition, we propose a novel analytical model to limit the complexity of studying the BSS operation, that can be exploited as a dimensioning tool for the BSS infrastructure. This model is proved to be effective in balancing QoS requirements, capital expenditures and operational cost in the planning and deployment of BSS systems. Differently from the work presented in [6], in our study the proposed queuing model is employed with the twofold objective of (i) properly dimensioning the BSS based on EV battery charging demand, QoS requirements, and possible cost and feasibility constraints, and (ii) performing a financial analysis that also includes capital expenditures for the BSS installation, besides the operational cost. Combining the contribution of renewable energy to power BSSs with a proper system dimensioning to trade off cost and QoS requirements, our study results effective in promoting the achievement of sustainability goals for a green and feasible deployment of urban mobility.

This study extends our previous paper [5], in which we began to study via simulation the potential of a BSS equipped with a set of photovoltaic panels, investigating the issue of properly dimensioning its capacity in terms of number of sockets and the sizing of the RE supply to satisfy the battery swapping demand, trading off cost, Quality of Service and feasibility constraints. Furthermore, the potential benefits of smart scheduling strategies for battery recharging were analyzed in [5]. With respect to our previous work, the main novel contributions presented in the current manuscript consist in the following:

- with respect to our previous study conducted via simulation, we now introduce an M/G/C/C queuing model to represent the BSS operation, extensively validating its capability to accurately reproduce the system behavior and the operational cost under realistic traffic demand;
- we explore the potentiality of the proposed stochastic model as a practical planning tool that can be flexibly adopted by the battery swap service

provider to dimension the BSS system, meeting cost and QoS constraints, without the need for performing time-consuming simulations;

- we thoroughly expand the analysis of the performance of Battery Swap technology in terms of cost and Quality of Service. In particular, with respect to [5], the dimensioning of the BSS in terms of number of sockets is more extensively investigated and discussed, to satisfy the battery swapping demand trading off cost and missed service probability;
- differently from our previous work, that only considered operational cost due to the energy bought from the electric grid, both capital and operational expenditures are now included in the cost evaluation, considering the capital expenditures for the BSS infrastructure and for the chargers installed at the BSS; furthermore, besides the cost for the energy bought from the grid, operational expenditures now include also the management cost due to the replacement of the EV batteries at the end of their lifetime.

The paper is organized as follows. After discussing related work in Sec. 2, we present the considered scenario and formulate the problem in Sec. 3. The model is proposed in Sec. 4 and validated in Sec. 5. Preliminary system dimensioning including renewable energy supply is discussed in Sec. 6. In Sec. 7, the model is applied to BSS system design and a comprehensive cost analysis is presented. Finally, Sec. 8 concludes the paper.

2. Related work

A raising interest is currently emerging in the literature around the potentiality of BSSs, as shown by several studies that investigate urban mobility scenarios based on electric vehicles and battery swapping technology. An overview of the possible architectures and designs of BSSs is provided in [4], along with an analysis of the standardization deployment and technical challenges of BSS systems. The survey in [7] details the state-of-the-art BSS literature and related business models, also reviewing hybrid scenarios that jointly combine BSSs and traditional charging stations. Focusing on the issue of planning BSS systems, authors in [8] propose a site selection framework for the BSS based on a Multi-criteria decision making method. In [9] a novel robust decision-making tool is presented to tackle the location selection problem for BSSs considering sustainability criteria. The work in [10] proposes a model to optimize both the BSS allocation and the number of batteries provided to users of electric scooters based on the battery

swapping demand. Other studies focus on the management and operation of BSS systems [11]. In [12] an algorithm is proposed to perform dynamic routing of a fleet of EVs belonging to a taxi service, to effectively serve customers, trading off delay constraints, the need for taxi detouring, and system cost. The work in [13] analyzes an hybrid scenario where a dynamic programming model incorporating a Markov decision process is applied to optimally distribute electric taxi batteries between a BSS and a traditional battery charging station, based on demand, electricity cost, and Quality of Service requirements. Various papers investigate optimal battery charging schedule approaches aiming at optimally satisfying the EV battery charging demand and minimizing the operational cost. Authors in [14] proposes a mathematical model to schedule the battery charging process. This approach optimizes an objective function that considers: (i) the number of batteries taken from the BSS to satisfy the demand for EV battery replacement, (ii) the potential damage due to high-rate charging, and (iii) the varying electricity cost. The work presented in [15] focuses on deploying a mathematical model to optimally operate a BSS considering the random demands of fully charged batteries, and exploiting demand shifting and energy sellback to reduce the BSS operational cost. In [16] and [17] optimal battery charging algorithms are proposed to identify the optimal battery charging schedule, with the purpose of maximizing the net profit of BSS and grant Quality of Service (QoS) requirements, based on a constraint Markov decision process. The study in [18] addresses the optimization scheduling problem in a Battery swapping-charging system exploiting Multi-Agent Deep Reinforcement Learning, whereas a Multi-Agent Deep Neural Network is deployed in [19] to reduce operational costs through optimal battery charging scheduling. The work in [20], based on a Monte Carlo simulation approach, shows that optimal schedule for the charging process contributes to satisfy more EV swapping and charging requests maximizing the service capacity. In [6] a queuing model is deployed to analyze the profit that can be achieved by a multi-service EV charging station through scheduling approaches, possibly powered by renewable energy. Our previous work [5] investigates different smart charging scheduling strategies to dynamically postpone the charging process of a variable fraction of batteries connected to a renewable powered BSS, with the aim of conveniently reducing the operational cost and enhancing the renewable energy utilization, still granting an acceptable Quality of Service. Regarding renewable powered BSSs, the study in [21] proposes a novel strategy to identify the optimal location of both traditional and swapping charging stations, in a scenario in which photovoltaic and wind energy sources are included as power supply. Authors in [22] introduce a multi-objective method for optimal operation of a centralized bat-

tery swap charging system where solar energy is integrated. In [23], a charging strategy is designed with the purpose of improving self-utilization of renewable energy. Forecasting models based on statistics and machine learning techniques can be integrated in the scheduling approaches to address the uncertainties related not only to traffic load and swapping demand, but also to renewable energy generation and weather conditions [24, 25].

Some studies investigate the impact of charging scheduling schemes on the system performance and on the required BSS dimensioning. Authors in [17] propose an optimal charging operation policy based on a constrained Markov decision process, to minimize the charging cost. The impact of the number of chargers on the system performance in terms of cost is investigated, nevertheless only the operational cost due to the energy bill is considered and the analysis is conducted via simulation. In [6] an M/M/C/C model is adopted to analyze the system performance of EV charging stations, including BSSs, under a scheduling algorithm that aims at optimizing the profits at the presence of random variables, such as electricity price, solar power, and battery state of charge. However, the study does not specifically focus on the problem of dimensioning the charging station, and operational cost due to battery replacement at the end of their lifetime as well as capital expenditures are not considered.

Despite the extensive research efforts in the literature to investigate the optimal operation of BSSs, trading off cost and QoS, only few studies are available specifically focusing on the dimensioning of BSSs and taking into account cost and QoS requirements, tasks that require a careful investigation of the EV based transportation demand [32]. To better highlight the research gaps and the contributions of our paper, Table 1 reports and compares the most recent studies available in the literature that specifically address the issue of dimensioning BSSs, possibly powered by RE. Most studies consider the case of BSSs to serve electric buses [27, 28, 31, 20], few works consider BSSs for long-haul trucks [26] or scooters [29], whereas our study differs for focusing on the case of small EVs that are typically adopted for car sharing or good delivery services. Some papers consider the integration of RE to power EVs. In particular, few studies investigate scenarios in which the RE is derived from microgrids [27] or nanogrids [31, 30]. In similar scenarios, microgrids and nanogrids provide supply to the Battery Energy Storage System (BESS), from which the battery units, once recharged, can be delivered to the BSS to serve EVs. Only few studies specifically address the case of a BSS equipped with a dedicated local RE supply [28, 29], like in our paper. Although these two studies investigate the dimensioning of the local RE supply, none of them analyzes the dimensioning of the BSS, whereas our work represents the only

Table 1: Studies in the literature focusing on the dimensioning of BSSs.

Study (Year)	EV type	Scenario	RE supply	Methodology	Sizing BSS	Sizing RE supply	OPEX		CAPEX
							for energy	for battery replacement	
Our study	Small EVs (car sharing, vans)	RE powered BSS	✓ (Local)	Markovian model, Simulation	✓	✓	✓	✓	✓
[26] (2024)	Long-haul trucks	Grid connected BSS		Mixed-Integer optimization	✓		✓		✓
[27] (2023)	Buses	BSSs in a Microgrid	✓ (Microgrid)	Mixed-Integer optimization	✓		✓		
[28] (2022)	Buses	RE powered BSS	✓ (Local)	Whale optimization algorithm		✓			✓
[29] (2022)	Scooters	RE powered BSS	✓ (Local)	COIN-OR optimization		✓	✓		✓
[30] (2019)	Generic EVs	Nanogrid based BESS and BSSs	✓ (Nanogrid)	Mixed-integer linear optimization	✓ (BESS)	✓			✓
[31] (2019)	Buses	Networked Nanogrids with BESS and BSSs	✓ (Nanogrid)	Mixed-integer linear optimization	✓ (BESS)	✓		✓	✓
[20] (2018)	Buses, taxis	BSSs and traditional charging stations		Monte Carlo simulations	✓		✓	✓	✓

study jointly considering the problem of sizing both the BSS and the local RE supply. Furthermore, whereas CAPEX are evaluated in most studies, only few papers consider the OPEX for the energy purchased from the electric grid [26, 27, 29, 20]. Our paper jointly assesses CAPEX and OPEX, balancing them with QoS requirements in terms of capability of meeting the EV swap demand. We remark that our study also provides an evaluation of the average OPEX per single EV swap service. Furthermore, in the OPEX analysis, only our study takes into account, besides the cost due to the electricity bill, the cost for battery replacement in the case of a renewable powered BSS. To this aim, we integrate the evaluation of battery lifetime considering the degradation due to the charging/discharging cycles that the storage units undergo during operation. Authors in [31] focus on the case of a nanogrid integrated BESS, also powered by RE. Although their dimensioning analysis includes the OPEX for battery replacement, this cost is estimated as a fixed fraction of the CAPEX for the battery units. In addition, the operational cost due to the energy bought from the grid is not considered. Management cost due to battery replacement is considered in [31], but the investigated scenario does not feature any RE supply. Finally, whereas most available studies focusing on the dimensioning of BSSs rely on Mixed-Integer optimization approaches, we propose a Markovian model to represent the BSS operation, offering a flexible tool to extensively investigate the trade off between the BSS dimensioning, cost, and the QoS, under realistic EV swapping demand and variable distributions of the battery charging levels upon EV arrivals at the BSSs. Our work yields useful insights on the sensitivity of the proposed model to variations of the traffic profiles that may occur in a real setup, hence, on the possible impact on the system dimensioning. To the best of our knowledge, currently no study offers a thorough analysis of the BSS dimensioning problem based on a stochastic queueing model, yielding a practical and easy-to-use analytical tool that can be exploited in the planning and deployment of renewable powered BSS systems, capable to address the issue of identifying the optimal number of required BSS sockets to satisfy the EV demand, trading off QoS requirements, capital investment and operational cost.

3. Sustainable urban mobility scenario

The considered scenario consists of a fleet of EVs owned by a private company either offering goods delivery service or car sharing service over a city and its suburban area, as in [5]. As depicted in Fig. 1, EVs are equipped with battery units that, once discharged, can be rapidly replaced at a Battery Swapping Station (BSS) by a fully recharged battery. Once the discharged battery is plugged to a

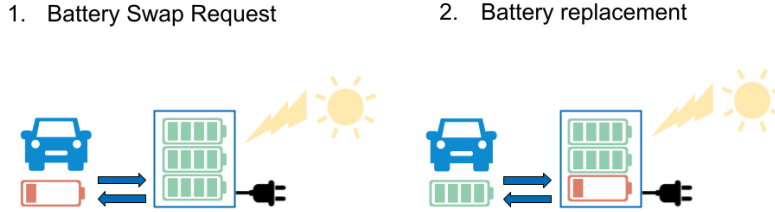


Figure 1: Renewable powered Battery Swapping Station [5].

BSS socket, its charging process can start. A 20 kWh capacity is assumed for each EV battery, compatible with the battery size of a small electric city car. Due to the nonlinear charging power of a lithium-ion battery unit, an exact estimation of its final charging time does not result easy [3]. However, a constant current can be used to recharge a battery until 80% of its full capacity has been achieved, whereas a significantly lower charging power is observed under higher State of Charge [33]. For an optimal recharging process, the maximum nominal charging rate is typically limited to $0.5 \cdot C_B$ per hour, where C_B is the nominal battery capacity [34]. In this work, we hence assume a constant charging rate of 10 kW, resulting in a full recharge of a drained battery taking two hours.

In an actual scenario, the company providing the Battery Swap service and the one offering the transportation service might coincide. The BS service is provided to EVs by means of a number of BSSs placed distributed in the considered urban area. Our study is performed focusing on a sample BSS, whose number of sockets is denoted by N_S . The energy required to recharge the battery units plugged at the BSS can be either drawn from the electric grid or derived from the RE that is locally produced by a set of photovoltaic (PV) panels (see Fig. 1). Considering one of the most efficient PV technology available on the market, we assume 19% charge efficiency. The PV module area occupancy required per kWp of capacity is about 5 m² [35, 36]. We adopt real RE generation profiles derived for the typical meteorological year in a Northern Italy city, based on the tool PVWatts [35]. For the BSS operational cost analysis, we adopt real electricity prices from the Day-Ahead Market, a dataset made publicly available by *Gestore dei Mercati*

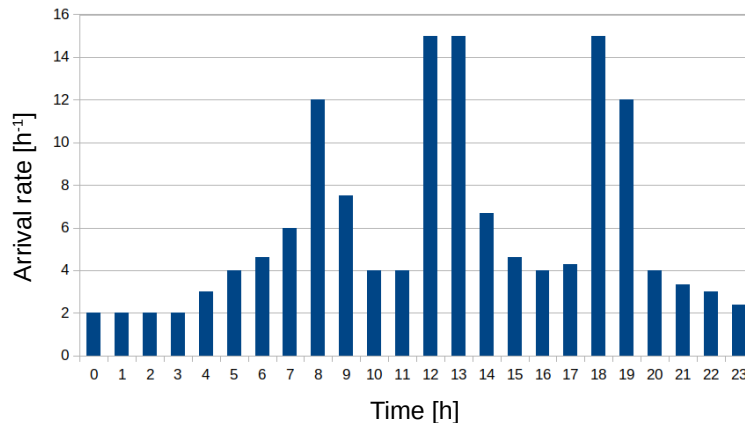


Figure 2: Daily profile of EV arrival rates [5].

Energetici (GME), the Italian company responsible for the electricity market management [37]. The arrivals of EVs at the BSS to swap their discharged battery are modeled by an inhomogeneous Poisson process, characterized by a mean arrival rate, λ , that varies depending on the hour of the day, following the daily traffic pattern depicted in Fig. 2 [5]. Real traffic profiles representing the daily variations of EV arrivals at traditional charging stations may not be suitable to properly represent the actual behavior of EV arrivals in a BSS system [38]. Indeed, the dynamics of the EV usage and of the battery charging process at the BSS may differ from those observed in a scenario with traditional EVs and charging stations, possibly leading to very different EV arrival patterns. However, real data about patterns of EV arrivals at a BSS in an urban scenario that result publicly available are difficult to be found in the literature. Hence, the considered EV arrival profile is derived taking inspiration from typical models adopted in the literature to represent arrival rates of EVs at traditional charging stations [39], accounting for a possibly different behavior in a BSS scenario, still obtaining a plausible pattern that exhibits traffic peaks at the beginning of the working day, during lunchtime, and in the evening, corresponding to the usual traffic variations observed during the day [5].

We denote $L \cdot C_B$ the charge level of the battery as the EV arrives at the BSS, with L corresponding to the fraction of the overall nominal storage capacity, i.e., C_B . L is assumed to be uniformly distributed according to $\mathcal{U}_{[L_{min}, L_{max}]}$, with $L_{min} \geq 0.2$. This latter assumption entails a battery Maximum Depth of Discharge (DoD) of 0.8, allowing to reduce degradation phenomena and improve the battery

lifetime. In addition, a relatively low value of L avoids the risk of fully running out of batter, so that an EV is granted the possibility to reach another BSS in case no storage units are currently ready for the battery swap at the considered BSS. Indeed, a fully recharged battery is used to replace the discharged storage unit of an EV upon its arrival at the BSS, and the EV battery takes its place at the corresponding BSS, hence beginning its recharge process. In case no fully recharged battery is available at the considered BSS, the EV cannot be served and another close by BSS must hence be reached.

4. BSS as an M/G/C/C system

We now introduce a queuing model to represent the BSS operation. A simplified analytical tool based on the model can be devised to dimension the BSS system, based on the actual traffic profiles, and respecting cost and QoS constraints.

The BSS can be modeled as an M/G/C/C queuing system, in which the EVs arrive according to a Poisson process, and the servers are represented by the $C = N_S$ sockets to which the batteries can be connected to be recharged. Since we assume a uniformly distributed battery charge level of the EVs upon arrival and a constant battery charging rate, which we denote μ , equal to $C_B/2$ [W], the charging time results uniformly distributed according to $\mathcal{U}_{[2L_{min}, 2L_{max}]}$ [h], with average value $2L$ [h]. No buffer is envisioned in this queuing system, indeed if an EV does not find a charged battery ready for replacement, the EV cannot be served and an alternative BSS must be found. As the BSS is modeled as an M/G/C/C system, the missed service probability, that we denote by P_l , can be derived according to the *Erlang B* formula [40], that allows to compute the proportion of arriving customers (i.e., EVs) that find all the C servers busy (i.e., all the $C = N_S$ sockets with a plugged battery still under charge) and cannot hence be served:

$$P_l = \frac{\frac{\rho^{N_S}}{N_S!}}{\sum_{i=0}^{N_S} \frac{\rho^i}{i!}} \quad (1)$$

where ρ corresponds to the mean load and it is derived as $\rho = \frac{\lambda}{\mu}$.

4.1. Key Performance Indicators

The Key Performance Indicators (KPIs) that are defined to evaluate the system performance are derived with the model in the following way. First, we identify a number of periods during the day in which the system operating conditions can

be considered stable. Then, for each period, the model is solved at the steady state and key performance indicators are derived. Finally, the performance indicators are averaged over the considered periods. These are the KPIs considered in what follows.

- a. *Average Service Loss probability - \hat{P}_l* : it is the average daily probability that an EV arrives at the BSS and cannot be served, since no battery is immediately ready to be swapped with the EV battery.

Via simulation, \hat{P}_l is computed as follows:

$$\hat{P}_l = \frac{1}{D} \sum_{i=1}^D \frac{V_i^a - V_i^s}{V_i^a} \quad i = 1, 2, \dots, D \quad (2)$$

where V_i^a is the number of EVs arrived at the BSS during day i , V_i^s is the number of EVs served by the BSS on day i , and D is the number of days in the observation period.

\hat{P}_l can be derived from the application of the queuing model presented in Section 4 as follows:

$$\hat{P}_l = \frac{1}{T} \sum_{i=1}^T P_{l_i} \quad i = 1, 2, \dots, T \quad (3)$$

where T is the number of time slots during a day, and P_{l_i} is the missed service probability derived from (1) considering the average arrival rate λ during time slot i .

- b. *Average Energy Demand from the Grid - E^G* : it is the average daily BSS energy demand drawn from the electric grid.

$$E^G = \frac{1}{D} \sum_{i=1}^D E_i^G \quad i = 1, 2, \dots, D \quad (4)$$

where E_i^G is the energy drawn from the grid on day i to recharge the batteries of EVs that are served during day i .

- c. *Average Total Cost - C^T* : it is the average daily cost to operate the BSS.

$$C^T = \frac{1}{D} \sum_{i=1}^D C_i^T \quad i = 1, 2, \dots, D \quad (5)$$

where C_i^T is the cost spent on day i to operate the BSS.

When the queuing model is applied, the value of C^T is estimated as follows:

$$C^T = \sum_{j=1}^T C_j^H \quad j = 1, 2, \dots, T \quad (6)$$

where C_j^H is the electricity cost time slot j , that is derived as:

$$C_j^H = p_j \cdot d_{EV} \cdot \lambda_j (1 - P_{l_j}) \quad (7)$$

where p_j is the electricity price during time slot i , $d_{EV} = \bar{L} \cdot C_B$ is the average energy demand to recharge an EV battery, λ_j is the average arrival rate at time slot j , and P_{l_j} is the service loss probability during time slot j .

A low value of C_T does not necessarily reflect a desirable system performance, since a high value of service loss probability may contribute to decrease the total cost at the price of Quality of Service impairment. We hence define also the following KPI, i.e. the *Average Cost per Service*, whose value is not influenced by the service loss probability.

- d. *Average Cost per Service* - C^S : it is the average daily cost to serve an EV and replace its battery with a recharged battery.

$$C^S = \frac{C^T D}{\sum_{i=1}^D V_i^S} \quad i = 1, 2, \dots, D \quad (8)$$

- e. *Overall Yearly Cost* - C^Y : it is the cost per year including both the capital expenditures for the BSS installation (CAPEX) and the operational cost (OPEX) due to the energy bought from the power grid during the BSS operation and to the management cost for replacing the chargers and the batteries at the end of their lifetime. Note that the cost for battery replacement is included in the computation of C^Y , since the considered scenario is based on the paradigm of *Battery-as-a-Service*. Indeed, the BSS system operator is the owner of the batteries, and the management cost for the replacement of a battery unit at the end of its lifetime is paid by the BSS operator.

This cost is computed as follows:

$$C^Y = \frac{C^F}{T^F} + \left(\frac{C^S}{T^S} + \frac{C^B \cdot C_B}{T^B} \right) \cdot N_S + C^T \cdot 365 \quad (9)$$

where C^F is the fixed cost for the BSS infrastructure installation, C^S is the cost for each of the integrated battery chargers, C^B is the cost per 1 kWh of battery capacity, whereas T^F , T^S and T^B correspond to the expected lifetime of the BSS infrastructure, of each charger and of each battery, respectively. Note that in our study we make the conservative assumption that $T^F = T^S$.

5. Queuing model validation

We now focus on the validation of the queuing model that is proposed in Section 4 to represent the BSS operation. We first investigate the model potential to accurately represent the system at the steady state. Second, we validate the model against the simulation results under the actual traffic profile. Furthermore, we investigate the capability of the model to capture the hourly variations of the service loss probability. Finally, we investigate the model capability to evaluate the BSS operational cost.

5.1. Evaluation at the steady state

To evaluate the capability of the proposed model to correctly represent the BSS operation at the steady state, the loss probability obtained from the queuing model is compared against the results obtained under simulation.

Fig. 3 reports the values of P_l derived from the model (red cross markers) along with those obtained under simulation (blue dot markers), for increasing number of sockets in the BSS, N_S . Each sub-figure corresponds to a different value of the inter-arrival time. As it can be clearly evinced from the graphs shown in the figure, the model is capable to very accurately represent the system behavior under any value of inter-arrival time. Under a very low inter-arrival time, as low as 1 min, P_l tends to be quite high even under large sized BSS, with the service loss probability decreasing almost linearly with the value of N_S . As the inter-arrival time increases, P_l tends to decrease exponentially as the number of sockets grows larger. As the inter-arrival time increases, the number of sockets required to minimize the service loss probability becomes smaller. For example, under $\lambda^{-1} = 5 \text{ min}$ more than 20 sockets are required to virtually avoid any service loss,

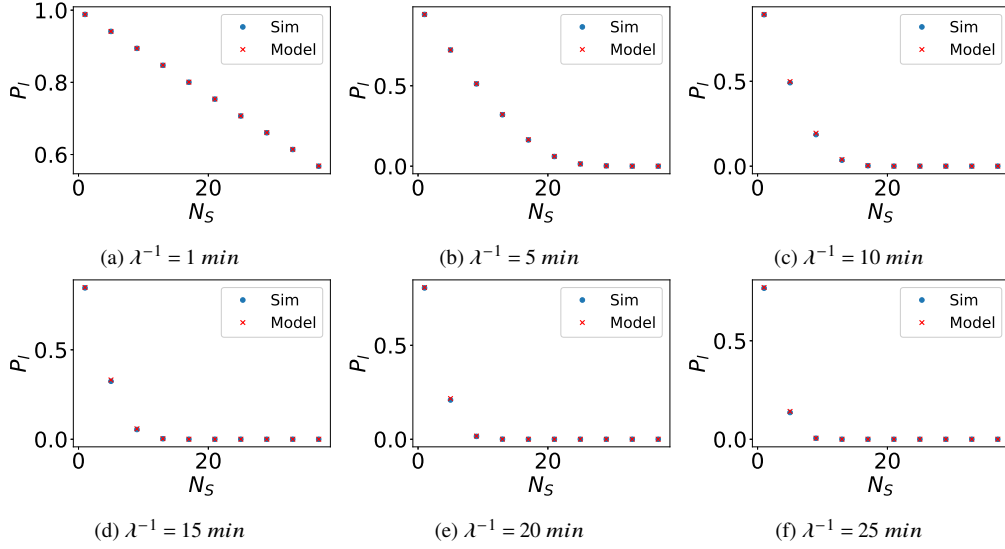


Figure 3: Service loss probability, P_l , versus number of sockets in the BSS, N_S , under the model and under simulation, for different values of average of inter-arrival time (λ^{-1}).

whereas less than 10 sockets are sufficient to guarantee a loss free service under a five-fold larger inter-arrival time.

The model is further validated considering different values of the average battery charging level of EVs upon arrival. Fig. 4 compares the values of P_l under the model (red cross markers) and under simulation (blue dot markers) for increasing values of N_S , considering different average values of L , hence different average values of the EV battery charging level upon arrival. Note that the actual charging level of the EV battery is derived as $L \cdot C_B$. We observe that even in this case the model accurately represents the BSS operation under any tested value of the average battery charge level. Clearly, given a value of N_S , if EVs arrive at the BSS to replace a battery whose charge level is on average at 30% of its full capacity, users experience a higher service loss probability with respect to the case in which the battery charge level upon arrival is half the overall capacity or more. According to the presented results, under $N_S > 25$ the system performance is similar in any case, featuring a negligible P_l regardless the considered value of L .

5.2. Applying the model under realistic traffic

We now apply the model to the actual trace of EV arrivals. To evaluate the model sensitivity to variations of the traffic profiles, besides the baseline traffic

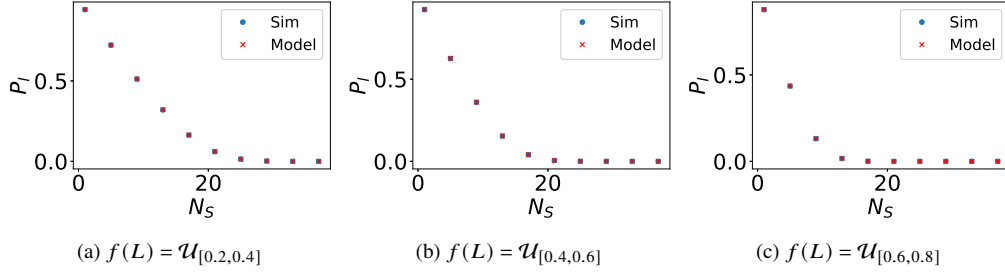


Figure 4: Service loss probability, P_l , versus number of sockets in the BSS, N_S , under the model and under simulation, for different values of average battery charging level of EVs upon arrival, $L \cdot C_B$.

trace we also consider traces derived from the original one introducing some random noise. Fig. 5 depicts the service loss probability, P_l , versus the number of sockets in the BSS, N_S , obtained under the model and under simulation, considering both the original traffic (Fig. 5a) and a derived trace that is obtained introducing some noise, denoted N_r , whose relative value with respect to the baseline trace is distributed according to $\mathcal{U}_{[-0.15,+0.15]}$ (Fig. 5b) and $\mathcal{U}_{[-0.3,+0.3]}$ (Fig. 5c), respectively. We observe that under lower size of the BSS the model tends to underestimate the service loss probability. No significant difference can be noticed in the model performance under modified traffic traces, even when the introduced noise is larger (Fig. 5c). The gap between the model and the simulation that is detected under small values of N_S can be likely explained by the fact that the average EV arrival rate may change as frequently as every time slot, i.e. every hour. Given the actual values of the arrival rate in the considered traffic trace (Fig. 2), that result lower than $20 h^{-1}$ even in peak periods, the time slot duration may not be sufficient to reach the steady state when the BSS is underdimensioned, hence resulting in fewer cases of missed service than expected. Nevertheless, overall the model looks quite effective in capturing the BSS behavior in terms of service loss probability under varying values of N_S .

5.3. Hourly variations of service loss probability

In order to further compare the model performance against simulation results, we provide a more detailed view on the model capability to catch the variations of P_l over the daytime. To this aim, Fig. 6 shows the daily profiles of the average service loss probability under different values of N_S , with 1 hour time steps, considering both the simulation (Fig. 6a) and the model (Fig. 6b). The absolute error given by the difference between model based service loss probability and

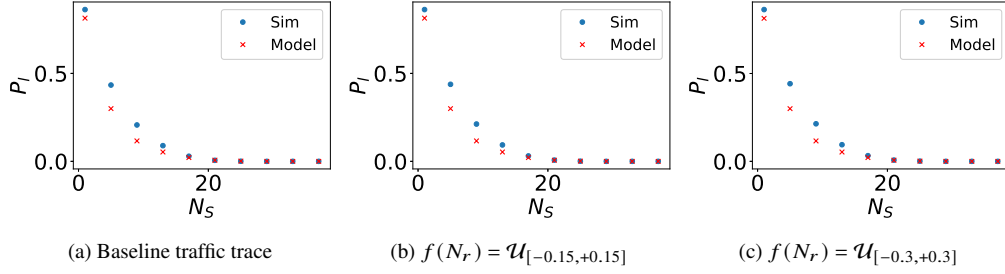


Figure 5: Service loss probability, P_l , versus number of sockets in the BSS, N_S , under the model and under simulation, considering the baseline traffic trace (a) and traffic profiles that are derived introducing some noise, N_r , distributed according to $\mathcal{U}_{[-0.15,+0.15]}$ (b) and $\mathcal{U}_{[-0.3,+0.3]}$ (c).

simulation derived values is reported in Fig. 6c. When less than 20 sockets are envisioned, we observe P_l peaks during those time slots in which the EV arrival rate is higher. Nine sockets are sufficient to guarantee an acceptable QoS at least during off peak time slots. Nevertheless, 21 sockets are required to grant a service loss probability lower than 0.05 during peak periods. Higher values of N_S provides negligible service loss probability over the entire daytime. The plot in Fig. 6c highlights how, under smaller size of the BSS, the largest gaps between the model and the simulation based results are observed during the traffic peaks. Indeed, in those time slots the BSS cannot fully satisfy the EV demand and some losses are detected. However, since the arrival rate may change every hour, the steady state may not be achieved over the course of a time slot, hence resulting in a slight decrease of the model accuracy in capturing the system behavior and in the estimation of the service loss probability under low values of N_S .

Note that the curve for $N_S = 21$ corresponds to the best dimensioned BSS among the tested sizes that guarantees an overall $P_l < 0.01$, ensuring less than 0.05 service loss probability during traffic peaks.

5.4. Model validation for cost analysis

A cost analysis based on the proposed model is now performed and compared against the cost derived via simulation. The related results are depicted in Fig. 7.

The average daily cost obtained under the model (red crosses) are compared against those derived from the simulation (blue dots) for several values of N_S , as shown in Fig. 7a. The average daily cost tends to increase as the BSS size becomes larger, with a faster ascent for lower values of N_S . Indeed, when additional sockets are included in an underdimensioned BSS, a relevant impact is detected on decreasing the operational cost, due to the higher number of EVs that can be

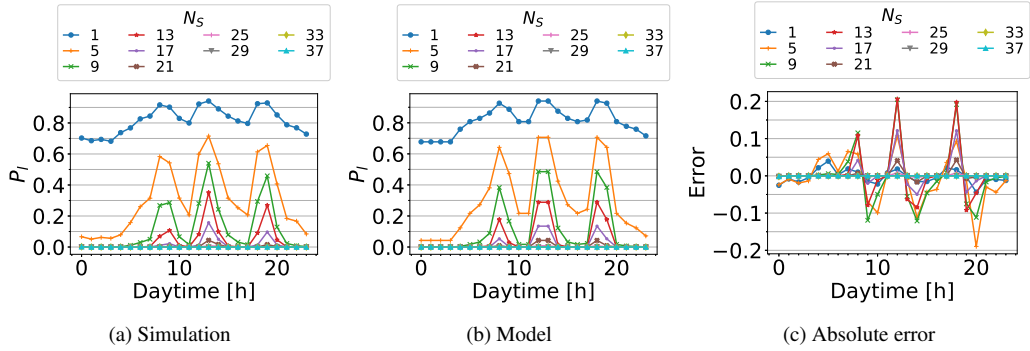


Figure 6: Average service loss probability, P_l , during the daytime for different number of sockets in the BSS, N_S , and under simulation (a) and under the model (b), with corresponding absolute error (c).

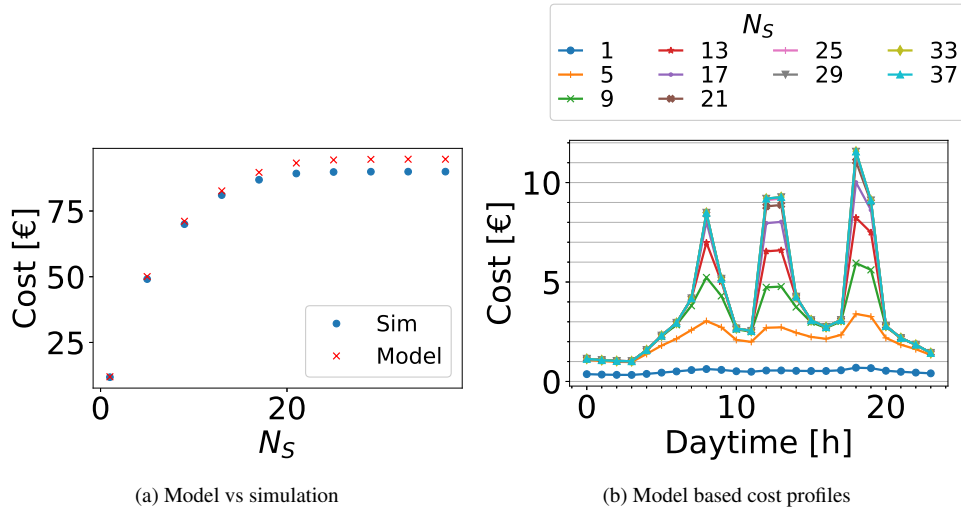


Figure 7: Model based average daily cost compared against simulation cost (a) and model based cost profile during the daytime (b) for different number of sockets in the BSS, N_S .

served. The model correctly represents the operational cost when the number of sockets is lower, whereas under high values of N_S , that achieve the highest QoS levels, the cost is only slightly underestimated by the model.

For completeness, Fig. 7b details the daily profiles of the operational cost under several values of N_S . Clearly, higher hourly costs are observed during traffic peak periods, when more EVs are served by the BSS.

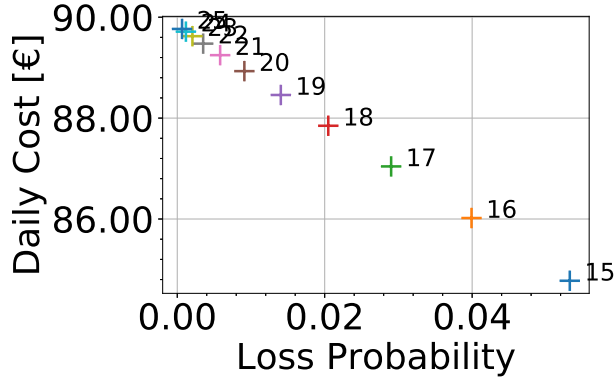


Figure 8: Average daily total cost versus loss probability, for different values of N_S , indicated by the labels.

6. Including renewable energy supply in the performance analysis

We now analyze how the BSS sizing, both in terms of charging capability, i.e. number of sockets, and RE supply capacity. The system is simulated over one year, assuming about 102 EV daily arrivals and a uniform distribution for L , according to $\mathcal{U}_{[0.2,0.4]}$.

6.1. Dimensioning the BSS

Considering the case without any RE supply, Fig. 8 shows the mean daily cost, C^T , versus the service loss probability, P_l , for several values of N_S , the number of BSS sockets. The labels in the plot indicate the corresponding value of N_S for each point in the graph. As N_S grows larger, the service loss probability is reduced at the price of a higher total cost, since progressively more vehicles can be successfully served. Nevertheless, this trend tends to become less evident for very large BSS sizes. Whereas BSS size of $N_S = 15$ results in a service loss probability of 0.05, expanding the BSS with only two sockets almost halves P_l , with an almost negligible price raise. Conversely, adding a socket to a BSS featuring $N_S = 22$, does not remarkably decrease the value of P_l , resulting lower than 0.01 under both BSS sizes. Conversely, a value of C^S of about 0.9 € (results not reported for the sake of brevity) is constantly observed under any BSS size, meaning that the overall cost reduction yielded by a lower BSS size actually depends on a limited capability to successfully serve EVs, reflected by a higher missed service probability.

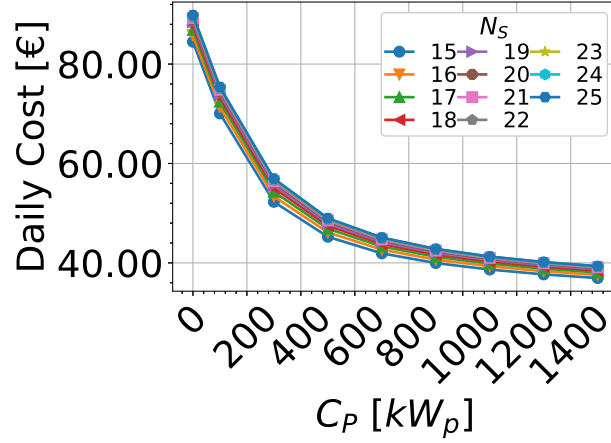


Figure 9: Average total cost, C^T , under different settings of PV panel capacity, C_P , and number of sockets, N_S .

6.2. Proper sizing of RE supply to reduce cost

We now assume that the BSS can jointly be powered by the electric grid and by the photovoltaic panel derived RE, focusing on the impact of the dimensioning of RE supply on the operational cost.

The mean daily cost, C^T , is reported in Fig. 9 for increasing capacity of the RE supply, C_P . Each curve corresponds to a specific value of N_S . Equipping the BSS with a PV panel capacity of $300 kW_p$ determines a cost reduction of about 40%, whereas adding 50% of the PV capacity leads to an almost negligible cost reduction of only few percentage points. Considering the limited gain yielded in terms of cost saving, it may hence result not convenient to integrate additional capacity to a $300 kW_p$ RE generator. Moreover, a similar capacity represents a proper balance cost and feasibility constraints in terms of area occupancy, since a surface of about $5 m^2$ per kW_p of capacity is required to install PV panel modules. Finally, a slight decrease of N_S can contribute to further reduce operational cost in the RE powered BSS, although a remarkable downsizing of the BSS is not desirable, due to the higher price paid in terms of missed service probability.

7. Application of the model in designing battery swapping station systems

We now describe how the proposed model can be effectively exploited to properly dimension the BSS size, considering the EV traffic rate, capital and operational cost, and Quality of Service requirements in terms of service loss probabil-

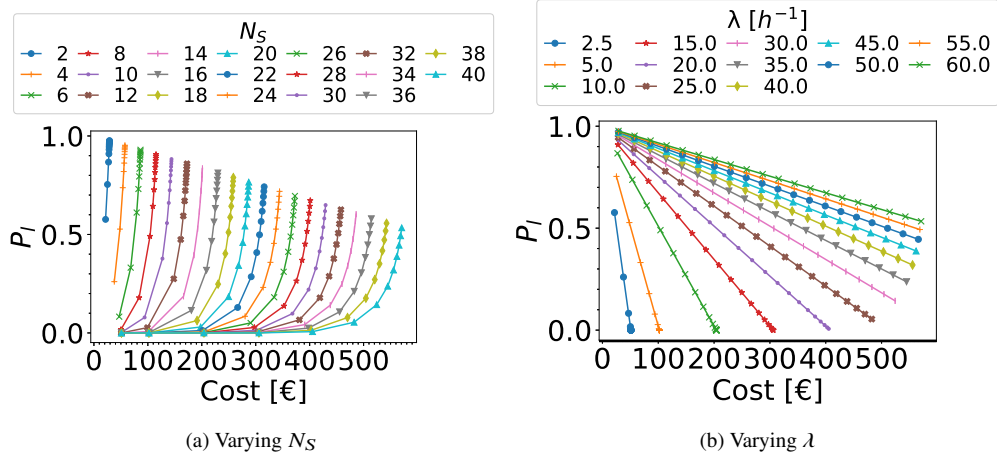


Figure 10: Model based service loss probability, P_l , versus average daily cost for different number of sockets in the BSS (a) and for several values of average arrival rates, λ (b).

ity. Furthermore, we also present how the model can be exploited to properly design BSS systems based on a cost analysis that includes both CAPEX and OPEX evaluation.

7.1. BSS dimensioning

Fig. 10 shows the values of the service loss probability, P_l , obtained from the model versus the average daily operational cost, considering several sizes of the BSS, N_S , and different EV arrival rates, λ . Each point in the subfigures represents a different combination of values of N_S and λ . Although Figs. 10a-10b represent the same set of results, data are shown grouped by N_S in Fig. 10a, whereas in Fig. 10b each curve corresponds to a different value of λ . Note that the operational cost C^T is derived according to (6), assuming an homogeneous Poisson process for arrivals. We can observe from Fig. 10a that under small values of N_S , the service loss probability P_l tends to rapidly grow, without significantly raising the cost. This is explained by the fact that the BSS cannot satisfy the battery swapping demand, hence limiting operational cost at the price of a remarkable QoS degradation. Under higher values of N_S , both P_l and cost increase as λ grows, showing a steeper ascent under low traffic demand. From the same results represented in Fig. 10b, it can be evinced that, for a given arrival rate, P_l decreases linearly with the raise of the number of installed sockets, hence determining a consequent increase of the operational cost, due to the largest number of EVs that can successfully be served by the BSS.

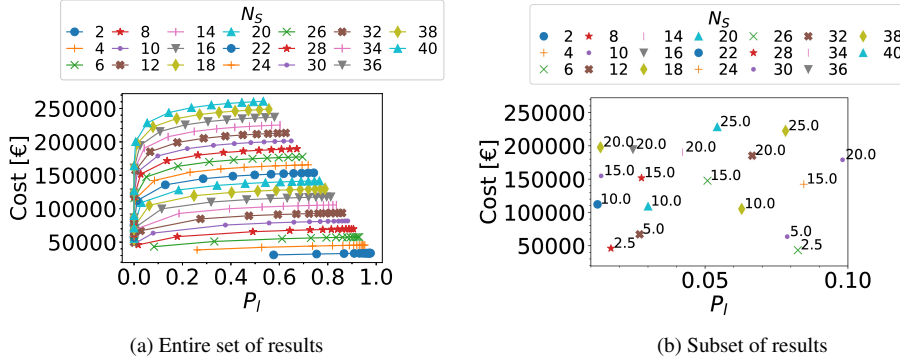


Figure 11: Average service loss probability, P_l , during the daytime for different number of sockets in the BSS, N_S , versus average yearly cost (CAPEX and OPEX). Subfigure (b) represents a subset of the results in subfigure (a), with labels representing the average inter-arrival time [m] corresponding to each point.

Our findings show that the proposed model can be effectively exploited as a practical tool to dimension a BSS system, based on the EV demand, the desired QoS requirements, and the cost constraints. For example, let us consider a traffic scenario characterized by an average EV arrival rate of $10 h^{-1}$. Assuming a target P_l lower than 0.05, 20 sockets are required at least to fully satisfy the defined requirement, still limiting the cost raise. Similarly, we could decide to dimension the system based on the target worst case P_l , taking into account the average EV arrival rate during the peak period and identifying the value of N_S needed to keep the service loss probability below the target threshold in that period of high EV charging demand. For example, setting a constraint on the worst case $P_l < 0.1$, and assuming a peak arrival rate of $20 h^{-1}$, 50% more sockets, i.e. $N_S = 30$, are needed to meet the desired service loss probability requirement.

The potential of a similar tool can be enhanced by integrating the evaluation of the impact of capital expenditures due to the installation of the required sockets in the BSS. The integration of this aspect to refine the proposed model is discussed hereafter.

7.2. Cost analysis including CAPEX

We now present a cost analysis that is performed based on the model, considering both CAPEX and OPEX, in order to take into account possible cost constraints on capital expenditure in planning and dimensioning a BSS system. CAPEX is computed considering both the fixed cost associated to the installation of the BSS baseline infrastructure and the cost for the BSS equipment, i.e. the chargers and

the batteries. A fixed cost, denoted C^F , of around 322800 € is estimated for installing a BSS, based on NIO statements [41]. The cost for each battery charger, C^S , is assumed to be 1200 USD (about 1100 €) [42], and the battery cost, C^B , is assumed to be 300 USD/kWh (about 280 €). We assume a 15 year lifetime, i.e. T^S , for each charger [43], and a battery lifetime, T^B , of 8 years [42].

Fig. 11a reports the average yearly cost (including CAPEX and OPEX) versus the service loss probability, P_l , for several values of N_S . Each point represents a different value of the EV inter-arrival rate. Several values of λ from 2.5 h^{-1} to 60 h^{-1} are evaluated. This graph shows that, under very small sized BSS, P_l results quite high even under low EV arrival rates and, while the service loss probability grows with the arrival rate, the cost is not affected, since the BSS capacity is saturated even under low service demand. When the number of sockets grows larger, under low service demand, P_l remains constant as λ increases, whereas the cost is raised. This means that the integration of further sockets in a well dimensioned system will affect capital expenditure without providing advantages in terms of QoS improvement. Conversely, when the arrival rate overpasses the BSS size capability, we observe increasing service loss probability along with a constant operational cost, since no additional EVs can be successfully served. Furthermore, the maximum value of service loss probability, observed under the highest arrival rate, tends to decrease linearly as N_S becomes higher, at the price of a cost increase.

Fig. 11b provides a detailed view of a subset of the results shown in Fig. 11a. In the reported graph, for each point a label highlights the value of the corresponding average inter-arrival time, λ^{-1} , expressed in minutes. Even in this case, the model results effective as a tool to properly dimension the BSS, either based on the average or peak BSS service demand, keeping into account not only QoS requirements and operational cost, but also the budget required for the initial BSS installation, that may significantly affect the decisions about the planning and sizing of the system. Considering the same practical example proposed in Section 7.1, a number of sockets equal to 30, although yielding a remarkable QoS level during peak traffic periods, may lead to relatively high cost for installing the BSS equipment. The BSS service operator may hence decide to pose additional constraints to limit the CAPEX. Note that, according to our findings, OPEX may account for 25% to 80% of the overall yearly cost, depending on the traffic demand and the BSS size. Furthermore, by conveniently relaxing the constraint on the maximum accepted service loss probability, a lower number of sockets can be installed in the BSS, allowing to decrease the overall cost (including CAPEX and OPEX) to satisfy the requirements set by the service operator.

8. Conclusion

Our study analyzes the potential of BS technology to enable a more sustainable urban mobility and to enhance the feasibility of e-mobility with respect to the advantages granted by traditional ICE based mobility. Our findings highlight how a proper sizing of the BSS capacity in terms of number of available sockets is necessary to limit the missed service probability. Furthermore, the integration of a RE supply of less than $20 kW_p$ per socket allow to decrease cost by almost 40%, making the BS technology more effective in providing a proper trade off between cost, sustainability and feasibility constraints.

Our study proposes a queuing model that accurately represents the BSS operation, providing a practical analytical tool that can effectively be employed during the planning and dimensioning of BSS systems in real scenarios, based on the actual EV battery swapping demand. Notably, this model allows to effectively trade off QoS requirements, capital expenditures for the installation of BSS infrastructure, management cost for battery and charger replacement at the end of their lifetime, and operational cost due to the energy bought from the electric grid.

As future work we plan to investigate more complex BSS scenarios that integrate additional RE sources, like wind energy, and smart charging scheduling strategies, to more effectively reduce the operational cost without impairing QoS. Furthermore, similar smart scheduling strategies can be conveniently coupled with properly designed energy management techniques, with the purpose of enhancing the interaction of the BSS with the Smart Grid in a Demand Response framework. Indeed, further cost reduction and additional revenues can be achieved by timely reacting to the requests issued by the Smart Grid to its customers to dynamically vary (increase or decrease) their energy demand. In this context, BSS operators can exploit the EV batteries under charge at the BSS as storage unit from which energy can even be drawn and injected to the electric grid when needed, and sell back to the Smart Grid any extra amount of RE that is not immediately used.

References

- [1] IEA, Key World Energy Statistics 2020, Tech. rep. (08 2020).
- [2] D. Pevec, J. Babic, A. Carvalho, Y. Ghiassi-Farrokhfal, W. Ketter, V. Podobnik, Electric Vehicle Range Anxiety: An Obstacle for the Personal Transportation (R)evolution?, in: 2019 4th International Conference on Smart and Sustainable Technologies (SpliTech), 2019, pp. 1–8.

- [3] H. Wu, A survey of battery swapping stations for electric vehicles: Operation modes and decision scenarios, *IEEE Transactions on Intelligent Transportation Systems* (2021) 1–23.
- [4] X. Chen, K. Xing, F. Ni, Y. Wu, Y. Xia, An electric vehicle battery-swapping system: Concept, architectures, and implementations, *IEEE Intelligent Transportation Systems Magazine* 14 (5) (2022) 175–194.
- [5] D. Renga, G. Centonze, M. Meo, Renewable powered battery swapping stations for sustainable urban mobility, in: *2022 IEEE International Smart Cities Conference (ISC2)*, 2022, pp. 1–7.
- [6] S. Esmailirad, A. Ghiasian, A. Rabiee, An extended m/m/k/k queueing model to analyze the profit of a multiservice electric vehicle charging station, *IEEE Transactions on Vehicular Technology* 70 (4) (2021) 3007–3016.
- [7] H. Wu, A survey of battery swapping stations for electric vehicles: Operation modes and decision scenarios, *IEEE Transactions on Intelligent Transportation Systems* 23 (8) (2022) 10163–10185. doi:10.1109/TITS.2021.3125861.
- [8] R. Wang, X. Li, C. Xu, F. Li, Study on location decision framework of electric vehicle battery swapping station: Using a hybrid mcdm method, *Sustainable Cities and Society* 61 (2020) 102149.
- [9] A. E. Torkayesh, M. Deveci, A multi-normalization multi-distance assessment (trust) approach for locating a battery swapping station for electric scooters, *Sustainable Cities and Society* 74 (2021) 103243.
- [10] M.-D. Lin, P.-Y. Liu, M.-D. Yang, Y.-H. Lin, Optimized allocation of scooter battery swapping station under demand uncertainty, *Sustainable Cities and Society* 71 (2021) 102963.
- [11] D. Cui, Z. Wang, P. Liu, S. Wang, D. G. Dorrell, X. Li, W. Zhan, Operation optimization approaches of electric vehicle battery swapping and charging station: A literature review, *Energy* 263 (2023) 126095.
- [12] H. R. Sayarshad, V. Mahmoodian, H. O. Gao, Non-myopic dynamic routing of electric taxis with battery swapping stations, *Sustainable Cities and Society* 57 (2020) 102113.

- [13] H. R. Sayarshad, V. Mahmoodian, An intelligent method for dynamic distribution of electric taxi batteries between charging and swapping stations, *Sustainable Cities and Society* 65 (2021) 102605.
- [14] H. Wu, G. K. H. Pang, K. L. Choy, H. Y. Lam, An optimization model for electric vehicle battery charging at a battery swapping station, *IEEE Transactions on Vehicular Technology* 67 (2) (2018) 881–895.
- [15] M. Mahoor, Z. S. Hosseini, A. Khodaei, Least-cost operation of a battery swapping station with random customer requests, *Energy* 172 (2019) 913–921.
- [16] H. Ko, S. Pack, V. C. M. Leung, An optimal battery charging algorithm in electric vehicle-assisted battery swapping environments, *IEEE Transactions on Intelligent Transportation Systems* 23 (5) (2022) 3985–3994.
- [17] B. Sun, X. Tan, D. H. K. Tsang, Optimal charging operation of battery swapping and charging stations with qos guarantee, *IEEE Transactions on Smart Grid* 9 (5) (2018) 4689–4701.
- [18] Y. Liang, Z. Ding, T. Zhao, W.-J. Lee, Real-time operation management for battery swapping-charging system via multi-agent deep reinforcement learning, *IEEE Transactions on Smart Grid* 14 (1) (2023) 559–571.
- [19] B. Aljafari, P. R. Jeyaraj, A. C. Kathiresan, S. B. Thanikanti, Electric vehicle optimum charging-discharging scheduling with dynamic pricing employing multi agent deep neural network, *Computers and Electrical Engineering* 105 (2023) 108555.
- [20] T. Zhang, X. Chen, Z. Yu, X. Zhu, D. Shi, A monte carlo simulation approach to evaluate service capacities of ev charging and battery swapping stations, *IEEE Transactions on Industrial Informatics* 14 (9) (2018) 3914–3923.
- [21] K. Balu, V. Mukherjee, Optimal allocation of electric vehicle charging stations and renewable distributed generation with battery energy storage in radial distribution system considering time sequence characteristics of generation and load demand, *Journal of Energy Storage* 59 (2023) 106533.

- [22] Y. Li, Y. Cai, T. Zhao, Y. Liu, J. Wang, L. Wu, Y. Zhao, Multi-objective optimal operation of centralized battery swap charging system with photovoltaic, *Journal of Modern Power Systems and Clean Energy* 10 (1) (2022) 149–162.
- [23] N. Liu, Q. Chen, X. Lu, J. Liu, J. Zhang, A Charging Strategy for PV-Based Battery Switch Stations Considering Service Availability and Self-Consumption of PV Energy, *IEEE Transactions on Industrial Electronics* 62 (8) (2015) 4878–4889.
- [24] H. Liu, Y. Zhang, S. Ge, C. Gu, F. Li, Day-Ahead Scheduling for an Electric Vehicle PV-Based Battery Swapping Station Considering the Dual Uncertainties, *IEEE Access* 7 (2019) 115625–115636.
- [25] J. Feng, S. Hou, L. Yu, N. Dimov, P. Zheng, C. Wang, Optimization of photovoltaic battery swapping station based on weather/traffic forecasts and speed variable charging, *Applied Energy* 264 (2020) 114708.
- [26] R. Wang, Y. Ju, Z. Allybokus, W. Zeng, N. Obrecht, S. Moura, Optimal sizing, operation, and efficiency evaluation of battery swapping stations for electric heavy-duty trucks, in: *2024 American Control Conference (ACC)*, 2024, pp. 707–712.
- [27] M. C. Kocer, A. Onen, J. Jung, H. Gultekin, S. Albayrak, Optimal location and sizing of electric bus battery swapping station in microgrid systems by considering revenue maximization, *IEEE Access* 11 (2023) 41084–41095.
- [28] T. Boonraksa, P. Boonraksa, B. Marungsri, W. Sarapan, Optimal PV Sizing of the PV-Based Battery Swapping Stations on the Radial Distribution System using Whale Optimization Algorithm, in: *2022 International Conference on Power, Energy and Innovations (ICPEI)*, 2022, pp. 1–4.
- [29] V. B, A. G. Kumar, Optimal sizing and operation of solar pv powered ev battery swapping station for indian petroleum retail outlet, in: *2022 Third International Conference on Intelligent Computing Instrumentation and Control Technologies (ICICICT)*, 2022, pp. 442–447.
- [30] M. Ban, D. Guo, J. Yu, M. Shahidehpour, Optimal sizing of PV and battery-based energy storage in an off-grid nanogrid supplying batteries to a battery swapping station, *Journal of Modern Power Systems and Clean Energy* 7 (2) (2019) 309–320.

- [31] M. Ban, M. Shahidehpour, J. Yu, Z. Li, A Cyber-Physical Energy Management System for Optimal Sizing and Operation of Networked Nanogrids With Battery Swapping Stations, *IEEE Transactions on Sustainable Energy* 10 (1) (2019) 491–502.
- [32] I. Pavić, N. Holjevac, M. Zidar, I. Kuzle, A. Nešković, Transportation and power system interdependency for urban fast charging and battery swapping stations in Croatia, in: *2017 40th International Convention on Information and Communication Technology, Electronics and Microelectronics (MIPRO)*, 2017, pp. 1465–1470.
- [33] H. Wu, G. K. H. Pang, X. Li, A realistic and non-linear charging process model for parking lot's decision on electric vehicles recharging schedule, in: *2020 IEEE Transportation Electrification Conference Expo (ITEC)*, 2020, pp. 2–7.
- [34] V. M. B. Pereira, J. O. De Sousa, G. C. Fonseca, R. N. Santos, An Automated Framework for Lithium Battery State of Health (SOH) Analysis, in: *2023 IEEE 8th Southern Power Electronics Conference and 17th Brazilian Power Electronics Conference (SPEC/COBEP)*, 2023, pp. 1–8.
- [35] A. P. Dobos, *PVWatts Version 5 Manual*, 2014.
- [36] M. Dalmaso, M. Meo, D. Renga, Radio resource management for improving energy self-sufficiency of green mobile networks, in: *Performance Evaluation Review*, Vol. 44, 2016, pp. 82–87.
- [37] Gestore Mercati Energetici, <https://www.mercatoelettrico.org/En/download/DatiStorici.aspx>, [Online; accessed 22 September 2021].
- [38] Z. Wang, P. Jochem, W. Fichtner, A scenario-based stochastic optimization model for charging scheduling of electric vehicles under uncertainties of vehicle availability and charging demand, *Journal of Cleaner Production* 254 (2020) 119886.
- [39] S. Park, A. Pröbstl, W. Chang, A. Annaswamy, S. Chakraborty, Exploring planning and operations design space for EV charging stations, in: *Proceedings of the 36th Annual ACM Symposium on Applied Computing, SAC '21*, Association for Computing Machinery, New York, NY, USA, 2021, p. 155–163.

- [40] R. B. Cooper, Introduction to queueing theory, Macmillan, 1972.
- [41] N. Gibbs, Chinese EV maker Nio is open to sharing battery swap tech with other automakers, <https://europe.autonews.com/automakers/chinese-electric-car-maker-nio-would-share-battery-swap-tech-other-automakers>, [Online; accessed 12 January 2023] (2022).
- [42] J. Neubauer, A. Pesaran, A Techno-Economic Analysis of BEV Service Providers Offering Battery Swapping Services, Vol. 2, 2013.
- [43] T. Zeng, H. Zhang, S. Moura, Solving overstay and stochasticity in pev charging station planning with real data, IEEE Transactions on Industrial Informatics 16 (5) (2020) 3504–3514.